

We are IntechOpen, the world's leading publisher of Open Access books Built by scientists, for scientists

5,300

Open access books available

130,000

International authors and editors

155M

Downloads

Our authors are among the

154

Countries delivered to

TOP 1%

most cited scientists

12.2%

Contributors from top 500 universities



WEB OF SCIENCE™

Selection of our books indexed in the Book Citation Index
in Web of Science™ Core Collection (BKCI)

Interested in publishing with us?
Contact book.department@intechopen.com

Numbers displayed above are based on latest data collected.
For more information visit www.intechopen.com



Advanced Space Flight Mechanical Qualification Test of a 3D-Printed Satellite Structure Produced in Polyetherimide ULTEM™

Jonathan Becedas, Andrés Caparrós,
Antonio Ramírez, Pablo Morillo,
Esther Sarachaga and Almudena Martín-Moreno

Additional information is available at the end of the chapter

<http://dx.doi.org/10.5772/intechopen.79852>

Abstract

The aim of this work is to demonstrate the use of additive manufacturing with thermo-plastic material in the whole functional structure of spacecraft and to mechanically qualify it for space flight. For such purpose, an 8 U CubeSat structure was manufactured in polyetherimide (PEI) ULTEM™ through 3D printing and passed several vibration tests. The results are compared with those obtained in the qualification of the same structure manufactured in aluminum alloy AA-6082 T651 through a conventional CNC method. The qualification consisted of passing the vibration requirements in quasi-static, sine, and random tests to fly in PSLV launcher. Finally, a robustness test for the 3D-printed structure is included, and all the results are analyzed. This study is being part of the H2020 European Project ReDSHIFT (Project ID 687500).

Keywords: polyetherimide, ULTEM™, vibration, space qualification, additive manufacturing, 3D printing, fused deposition modeling, satellite structure

1. Introduction

The cost of putting a satellite into orbit is directly related to its mass. Putting 1 kg into a low Earth orbit can be between \$10.000 and \$20.000 for medium- to large-sized satellites [1, 2] and between \$40.000 and \$50.000 for small satellites (under 100 kg) [3]. In small satellites one of the subsystems that most contribute to the total mass of the system is the structural subsystem. Normally, the structure of the satellite contributes between 30 and 40% to the total mass of the

spacecraft. However, this is normal because these structures are commonly made of metallic materials such as aluminum alloys [4], because they need to resist very demanding environmental conditions in space and very demanding mechanical conditions during the launch, and because they have to guarantee the integrity of the satellite itself and of the other satellites placed in the launcher.

However, additive manufacturing is enabling the use of new materials for space such as polyetherimide (PEI) [5]. Polyetherimide (PEI) is an amorphous thermoplastic very resistant to high and low temperatures, with a high glass transition temperature, and very resistant to mechanical loads [6] and has half the density of the aluminum. The incorporation of this type of materials in the structure of satellites can highly reduce the mass of the overall system and the cost of putting it into space.

Nevertheless, the incorporation of new materials and methods in a spacecraft requires a profound analysis and passing of very demanding tests to prove that it is qualified to be launched and to be performed with enough margin in the space environment [7]. During the launch, the structure will suffer extreme mechanical stress. The conditions are a combination of static and dynamic loads or mechanical aggressions [8] constituted by the static loads and acceleration, the pressure produced by the mechanical waves generated by the noise inside the launcher, and the vibrations produced by its motor and its structure, by all the other satellites onboard, and by the shocks when every stage of the launcher is separated or when the satellite is separated from the launcher. These effects are combined as a random vibration in which shocks can be superimposed.

In order to verify that a satellite can resist the launch, the launcher authorities provide a set of requirements that have to be fulfilled and verified through mechanical testing. These are modal survey vibration tests to identify the modes of vibration of the satellite to demonstrate that the main modes have higher frequencies than the launcher and that it will not enter in resonance, quasi-static vibration tests to demonstrate that the satellite resists the accelerations of the launcher, sine vibration tests to demonstrate that the satellite resists all the vibrations induced by the launcher, random vibration test to demonstrate that the satellite resists an emulated launch in which all the loads are combined, and shock vibration test to demonstrate that the satellite resists the shocks during the launch.

In this work, a small satellite structure 8 U CubeSat type 3D-printed in PEI ULTEM™ 9085 is presented. The structure was mechanically tested at qualification levels to fly in the Polar Satellite Launch Vehicle (PSLV) [9], and the results are presented compared with the results of the same structure manufactured in aluminum alloy AA-6082 T651 through a conventional CNC method. Once the structure in ULTEM™ was qualified, a robustness test was done to identify its mechanical limits. All the results are included in Section 3 and discussed in Section 4.

2. Materials and methods

The qualification of a new structural design for a spacecraft requires a very methodic procedure in which all the boundary conditions shall be considered and controlled with care:

manufacturing environment and methodology, transport of the parts and their inspection, assembly, testing, and analysis. The whole process shall be completely controlled and monitored. In this section, the experiment is described, the methodology applied in the whole process is introduced, the test specimens are detailed, and the instrumentation and equipment used during the testing are specified.

2.1. Experiment description

The objective of this experiment is to validate the use of additive manufacturing technology with PEI to be implemented in functional structures of satellites. For this purpose, a novel structure with 3D-printed PEI ULTEM™ 9085 was manufactured and tested, and it was compared with the same structure manufactured in aluminum alloy AA-6082 T651 with classical CNC milling methodology. The two test specimens are described in Section 2.1.1.

To qualify the structure of the spacecraft, a structural model was assembled as part of the model philosophy established [10]. The structural model was constituted by the structural subsystem of the satellite (functional structure) and by mass dummies, which were mechanically equivalent to the real components of the satellite.

2.1.1. Test specimen description

The test specimens used in the test campaign were two CubeSat structures manufactured by using different materials and technologies:

- Aluminum alloy AA-6082 T651, density 2.70 g/cm^3 , manufactured by CNC milling
- PEI ULTEM™ 9085, density 1.34 g/cm^3 , manufactured by fused deposition modeling (FDM)

The structural subsystem of the 8 U CubeSat consisted of six panels (cube faces), a T bracket, and a central avionics tray providing mechanical interface for all the equipment onboard the satellite. To validate the 3D-printed structure in ULTEM™, no particular design optimization was performed with regard to the structure in aluminum; in other words, the same set of manufacturing drawings and CAD models was used to manufacture the model in the machining workshop and in the additive manufacturing facility.

The design baseline was a medium-resolution Earth observation (EO) mission with the following commercial components constituting the satellite: an Astro Digital Data and Power Module (DPM), three Sinclair reaction wheels (RWs), a Sensor gyrometer (GYR), two BST Star Trackers (STs), a Syrlinks X-Band Transmitter Unit (XTU), a VACCO Propulsion System (PS), an ANTCOM GPS antenna (GPS), an SCS Space Gecko imager payload (IMG), an EnduroSat X-Band antenna, and an Astro Digital UHF antenna.

The internal distribution of the components in the internal volume of the 8 U structure was done by considering the center of gravity (CoG) requirements imposed by the launcher [11].

For the design of the structural models, the complete avionics suite was substituted by mass dummies or mock-up representative of their functional counterparts not only in terms of envelope and mounting interfaces (bolts) but also in mass and center of gravity (CoG). All replicas

were manufactured in aluminum and anodized to be preserved from corrosion. The total mass of mock-ups was 5.2 kg, considering a realistic configuration for an 8 U CubeSat. The structure in aluminum had a mass of 3.1 kg (37.35% of the total mass, which was 8.3 kg), and the structure in ULTEM™ had a mass of 1.45 kg (46.77% less mass than the aluminum structure and 21.80% of the total mass of the structural model, which was 6.65 kg). **Table 1** shows the list of mock-ups with the most relevant mechanical properties: dimensions, mass, and coordinates of the center of gravity with respect to the geometric center of the satellite structure.

The overall structure design adheres to the CubeSat standard [12], and it could be fitted in any commercial P-POD designed to host an 8 U satellite. **Figure 1** shows the parts of the structure made with additive manufacturing in PEI ULTEM™. **Figure 2** depicts the mock-ups assembled in the structure.

Figure 3 shows the two test specimens populated with the mock-up avionics. The single circular window (front pictures) provided field of view for the payload camera. The two orthogonal circular windows (back pictures) provided fields of view for the star trackers. The purpose of the overtures in the structure was to reduce the mass of the structure while providing access to manipulate inside the spacecraft during assembly activities.

2.1.2. Testing platform description

The testing platform was represented by an electrodynamic shaker model LDS B&K V850–440 with an LDS B&K LPT 600 slip table with a mechanical interface adapter mounted on it (see **Figure 4**). The electrodynamic shaker stood over a concrete block by means of four silent blocks. The shaker was controlled by an LDS-Dactron control system, and the signal was amplified with an LDS B&K SPA 32Kv3 Kk4a-CE amplifier of 22 kN. Three accelerometers

Tag	Equipment name	Mock-up dimensions (mm)	Mock-up mass (gr)	X CoG (mm)	Y CoG (mm)	Z CoG (mm)
DPM	Data and Power Module	100(W) × 199(L) × 87(H)	1796	64.9	−3.6	−55.0
IMG	Imager payload	97(W) × 96(W) × 60(H)	473	2.1	58.5	−53.9
GPS	GPS antenna	40(W) × 40(L) × 26(H)	41	−64.1	−7.3	−23.8
ST1	Star tracker No. 1	30(W) × 30(L) × 38(H)	233	0.9	−74.5	−23.8
ST2	Star tracker No. 2	30(W) × 30(L) × 38(H)	233	−57.0	−71.0	−17.6
RW1	Reaction wheel No. 1	50(W) × 50(L) × 40(H)	171	108.5	105.5	−113.1
RW2	Reaction wheel No. 2	50(W) × 50(L) × 40(H)	171	84.7	35.2	41.7
RW3	Reaction wheel No. 3	50(W) × 50(L) × 40(H)	171	−64.5	61.1	−43.6
GYR	Gyroscope	39(W) × 45(L) × 22(H)	51	40.9	41.6	−53.9
PRO	Propulsion	39(W) × 45(L) × 80(H)	1181	0.0	0.0	101.7
XTU	X-Band transmitter	90 (W) × 96(L) × 24 (H)	433	0.0	0.0	−101.7

Table 1. List of mock-ups with mechanical properties.

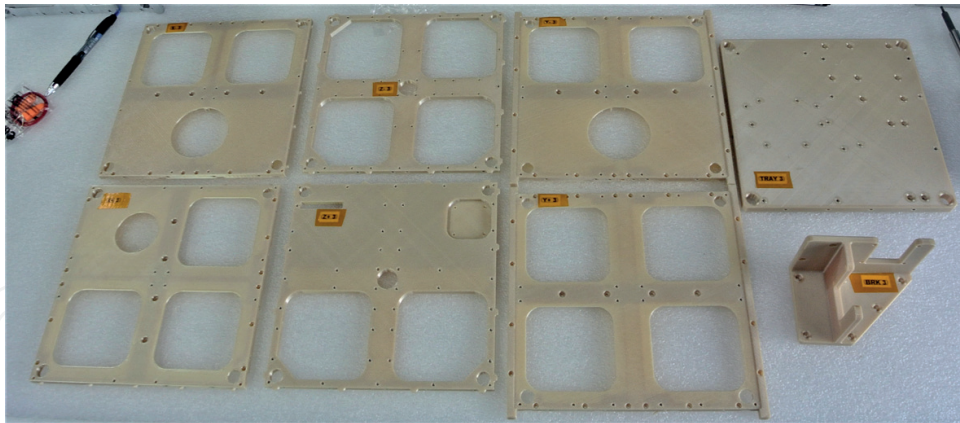


Figure 1. Structure of the 3D-printed satellite in PEI.

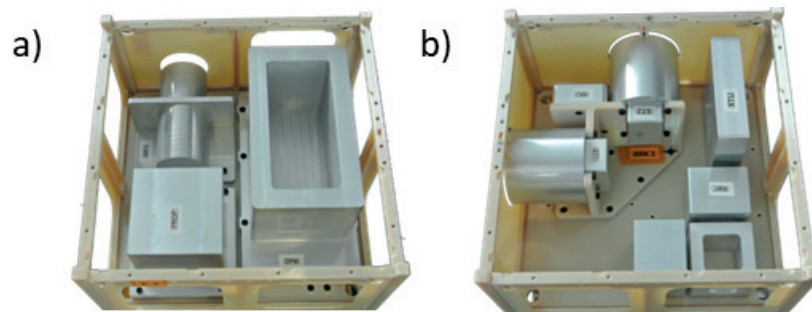


Figure 2. Mock-ups assembled in the 3D-printed structure. (a) Top view and (b) bottom view.

were used to record the measurements, one monoaxial 4513-B type used as control and two triaxial 4520-001 type for recording the response of the structural models.

2.1.3. Test specifications

The structural model was tested at qualification levels established by PSLV [11]. The applied loads to qualify the structure were the following:

- Modal survey: to identify the modes of the structural model, a modal survey was done. The parameters were the following: maximum test frequency (2 kHz) and sweep-type logarithmic and sweep rate (2.0 oct/min). This was done in every axis: X, Y, and Z.
- Quasi-static load (QSL): it was characterized by a ramp up which increases amplitude levels from 0.1 to 8.75 g of acceleration between 5 and 20 Hz, acceleration amplitude of 8.75 g at 20 Hz, and a ramp down from the maximum amplitude of 8.75 to 0.1 g at frequencies from 20 to 5 Hz. The load profile is shown in **Figure 5**. This test was done in every axis: X, Y, and Z.
- Sine load: with maximum acceleration amplitude of 2.5 g at frequencies from 10 to 100 Hz. The load profile is shown in **Figure 6**. This test was done in every axis: X, Y, and Z.

- Random load: it was defined by a specific power spectral density (PSD) profile in function of the frequency. The profile is defined in **Figure 7**. This test was done in every axis: X, Y, and Z.
- Shock load: it was modeled as a variable acceleration profile with levels between 8 and 220 g for frequencies between 20 and 2000 Hz, as shown in **Figure 8**. This test was done in axis Z. The profile from 30 to 300 Hz was representative of the qualification level; for higher frequencies, the test could not be done for limitations of the testing platform used. However, this test specification was representative enough.

The tests were done by following the standards [7, 10].

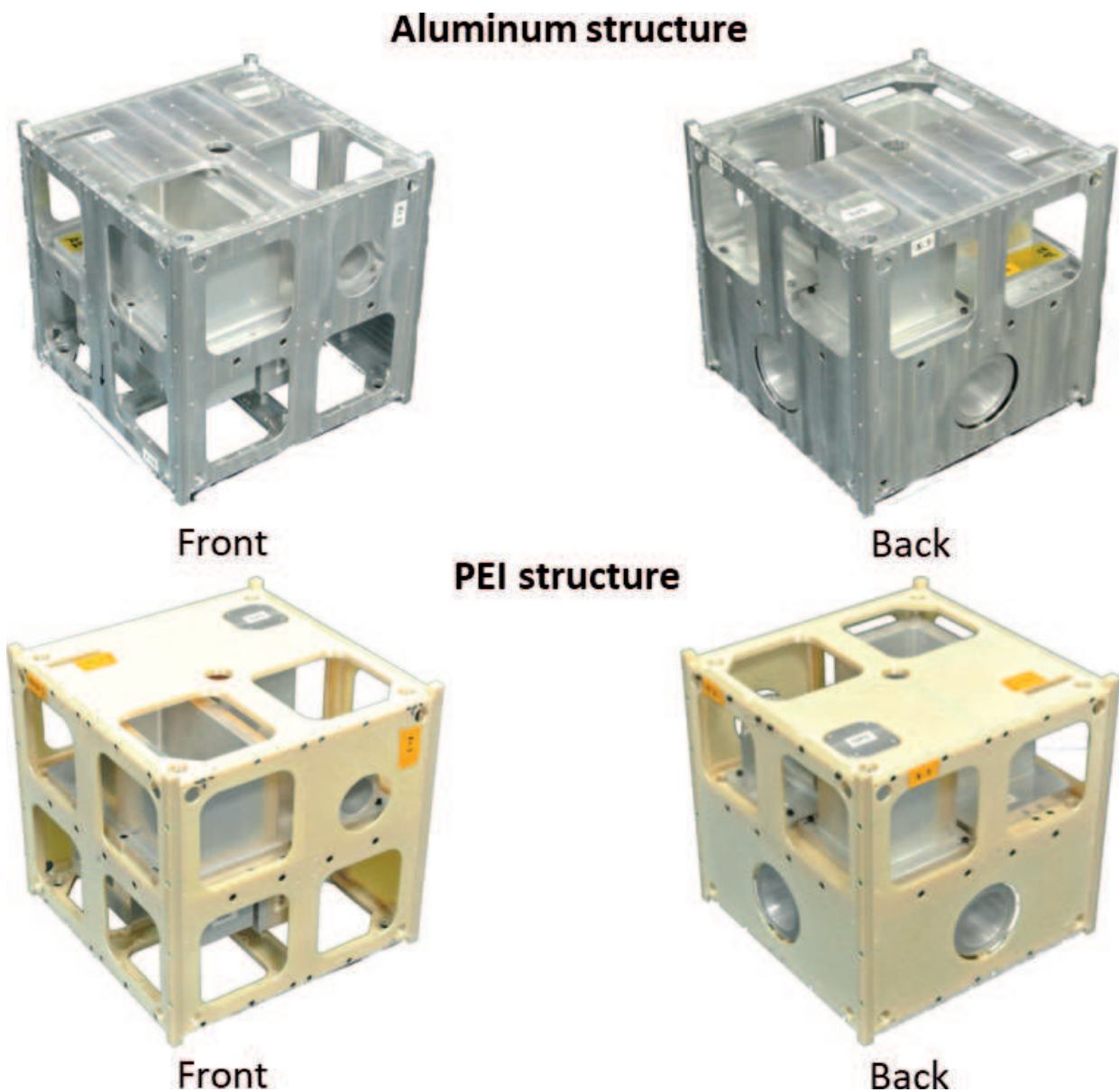


Figure 3. ReDSHIFT structural models.



Figure 4. Interface adapter mounted on the shaker slip table.

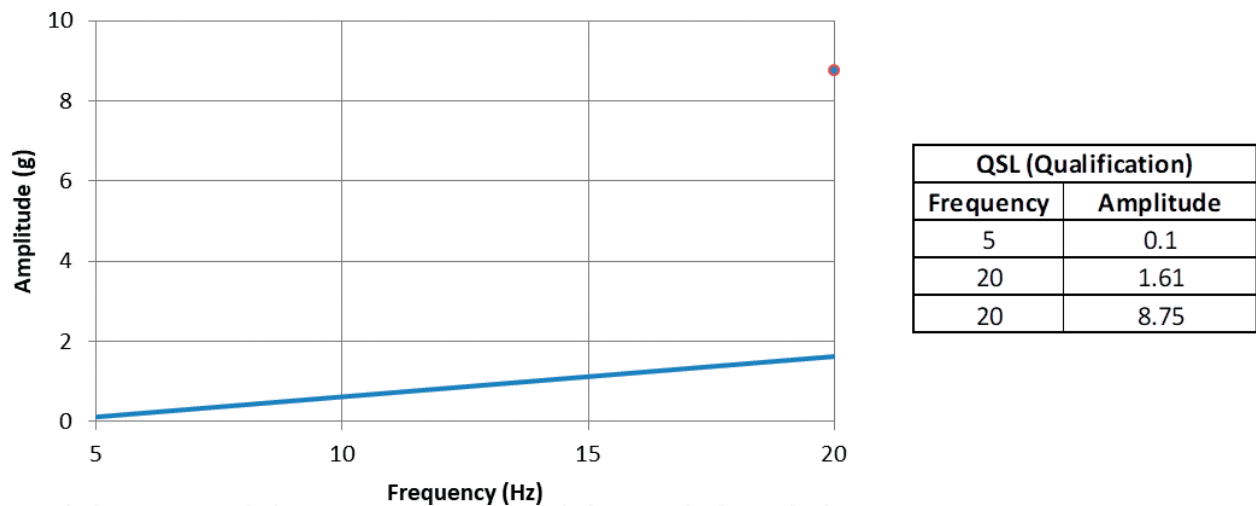
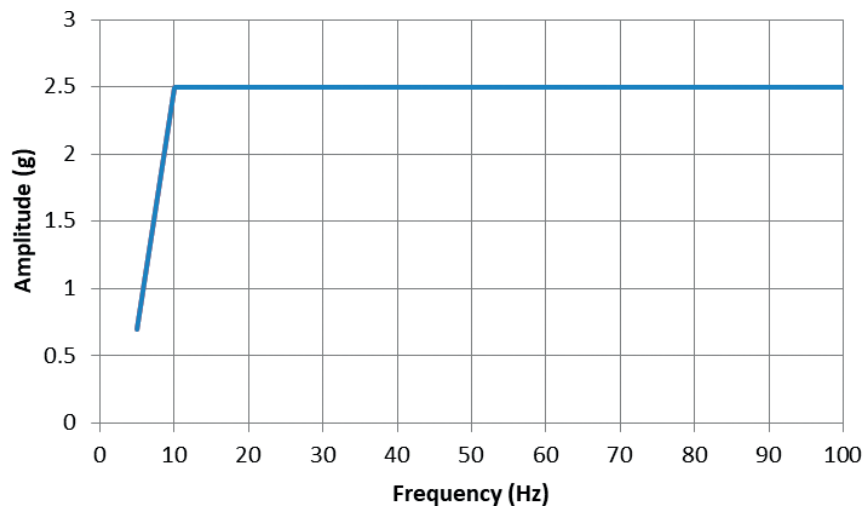


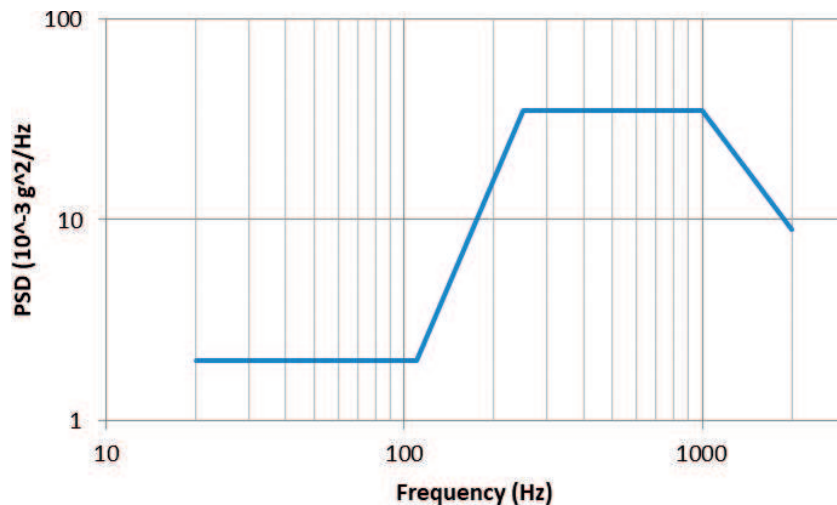
Figure 5. QSL profile.

As the purpose of the test was to qualify the 3D-printed structure and to analyze the differences between the 3D-printed ULTEM™ structure and the CNC-milled aluminum structure, the tests were performed on the bare structural models, i.e., not preserving the models inside a P-POD. For such a purpose, the bottom panels of the structures incorporated, near the corners, four M12 holes that were used to secure the test specimen on top of the mechanical interface with the slip table. In a real launch scenario, this would imply the adoption of pyro-bolts to assemble the spacecraft to the launcher interface. This was the worst case scenario for qualification purposes of the structure.



Sine Load (Qualification)	
Frequency	Amplitude
5	0.7
10	2.5
100	2.5

Figure 6. Sine load profile.



Random Load (Qualification)	
Frequency	PSD
20	2
110	2
250	35
1000	35
2000	9

Figure 7. Random load profile.

2.1.4. Experimentation methodology

To guarantee a representative experimentation for the qualification of the structural model in ULTEM™, a specific and very controlled process was carried out. It started with the selection of competitive providers to manufacture the parts. Once they were received, a careful incoming goods reception was done in order to validate that all the parts fulfilled the specifications defined. This process consisted of inspecting from the parcel to its content, taking into account physical status and functionality. A report (incoming inspection report) was done in order to register every detail related to packaging, labeling, wrapping, isolation, external damages, and internal damages. Serial and part numbers were checked. Photos were also taken so that every aspect could be graphically supported. After the approval of the incoming inspection, the structural model was assembled to validate the design and manufacturing processes. Once the assembly was successful, the structures were dismantled and protected, side panel by side

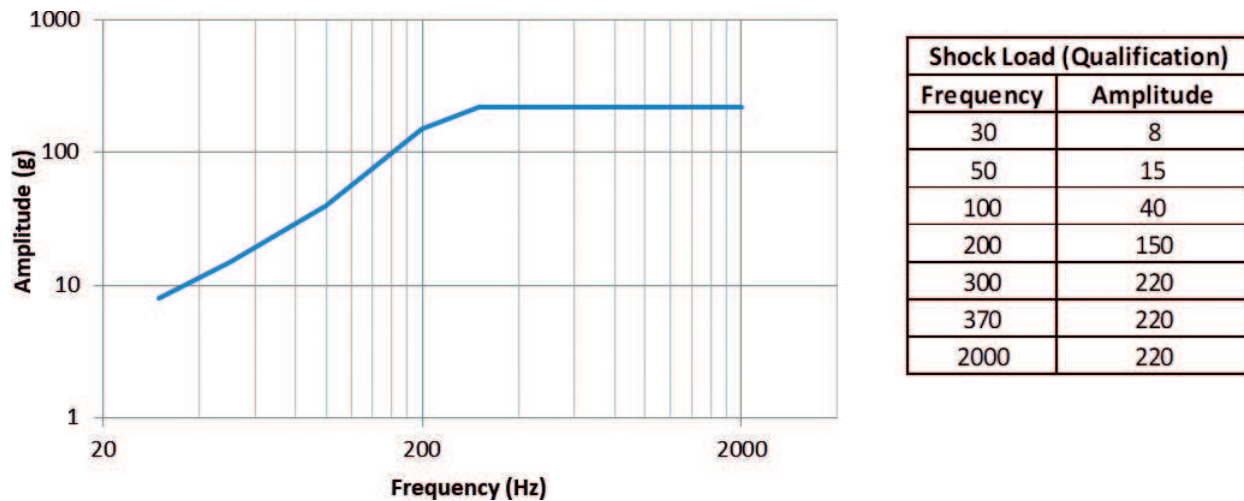


Figure 8. Shock load profile.

panel, with bubble wrap, and they were packaged using shock-absorbing material. The same process was carried out to package the mock-ups.

Then, the packaged parts and required tools were prepared to be sent to the test facilities. Transport documents (packing list and annexes) were prepared. These documents contained information such as shipper, addressee, item description, references, gross weight, net weight, dimensions, and Incoterms. Incoterm is reflected the International Commercial Terms, i.e., it specified who took what risk and where.

When the goods arrived at the test facilities, the incoming goods reception process started again, and a new incoming inspection report was carried out. Transport documents were also checked.

Once the incoming inspection report was favorable, the structural model was assembled and mounted on the interface adapter with the slip table of the shaker.

To carry the experiment out, the Z panel of the specimen was fixed on the interface adapter by means of four M12 screws; subsequently, the rest of the assembled structure was fit on the Z panel and fixed by means of 24 M2.5 screws. For X and Y axes, the test was performed on the slip table (horizontal configuration) just rotating the test specimen 90°. For the Z-axis experimentation, the electrodynamic shaker was rotated 90° to the vertical configuration (**Figure 9**).

The following testing procedures were followed:

1. Survey vibration test in the direction of the selected axis of the test specimen to detect the vibration modes
2. Sine vibration test in the selected axis of the test specimen at qualification level
3. Survey vibration test in the selected axis of the test specimen to detect if there were significant changes in the modes

4. QSL vibration test in the selected axis of the test specimen at qualification level
5. Survey vibration test in the selected axis of the test specimen to detect if there were significant changes in the modes
6. Random vibration test in the selected axis of the test specimen at qualification level
7. Survey vibration test in the selected axis of the test specimen to detect if there were significant changes in the modes
8. Shock vibration test only in the selected axis of the test specimen
9. Survey vibration test after the shock vibration test in the Z-axis of the test specimen to detect if there were significant changes in the modes

A significant change was defined as a change in frequency of the modes of at least 10%. Firstly, the CNC aluminum model was tested on the X-axis and then on the Y-axis. Secondly, the 3D-printed ULTEM™ model was tested on the X-axis and then on the Y-axis. Thirdly, the electrodynamic shaker was turned 90° to test on the Z-axis of the CNC aluminum model first, and then on the ULTEM™ model.

When the experiment was finished, the structures were dismantled and protected, side panel by side panel, with bubble wrap, and they were packaged using shock-absorbing material. The same process was carried out to package the mock-ups. The same logistics and inspection processes explained before were followed to transport the parts back.

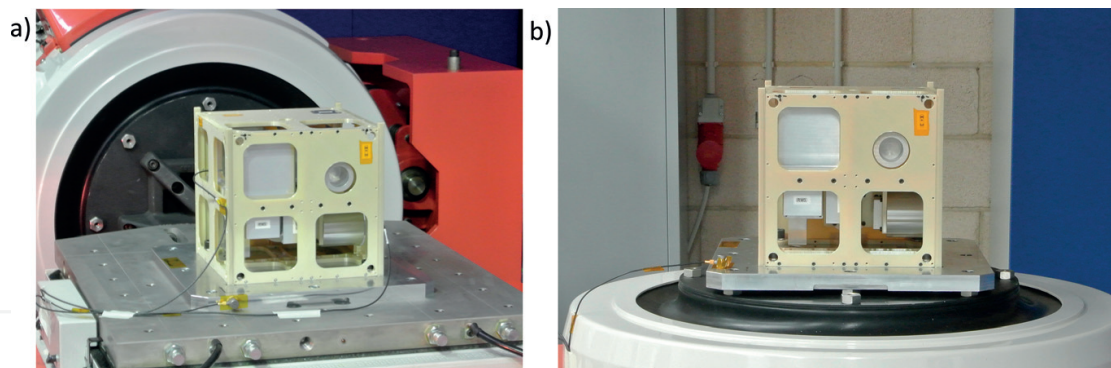


Figure 9. 3D-printed structural model mounted in the testing platform. (a) X-axis test and (b) Z-axis test.

3. Results

3.1. X-axis test results of the 3D-printed ULTEM™ structure

Figure 10 shows the results for the test carried out in the X-axis of the 3D-printed ULTEM™ structural model: modal survey (Figure 10(a)), QSL (Figure 10(b)), sine (Figure 10(c)), and random vibration (Figure 10(d)) tests. All the unities were expressed in g (9.81 m/s^2) except in the random test, which was expressed in PSD (power spectral density (g^2/Hz)). The red color

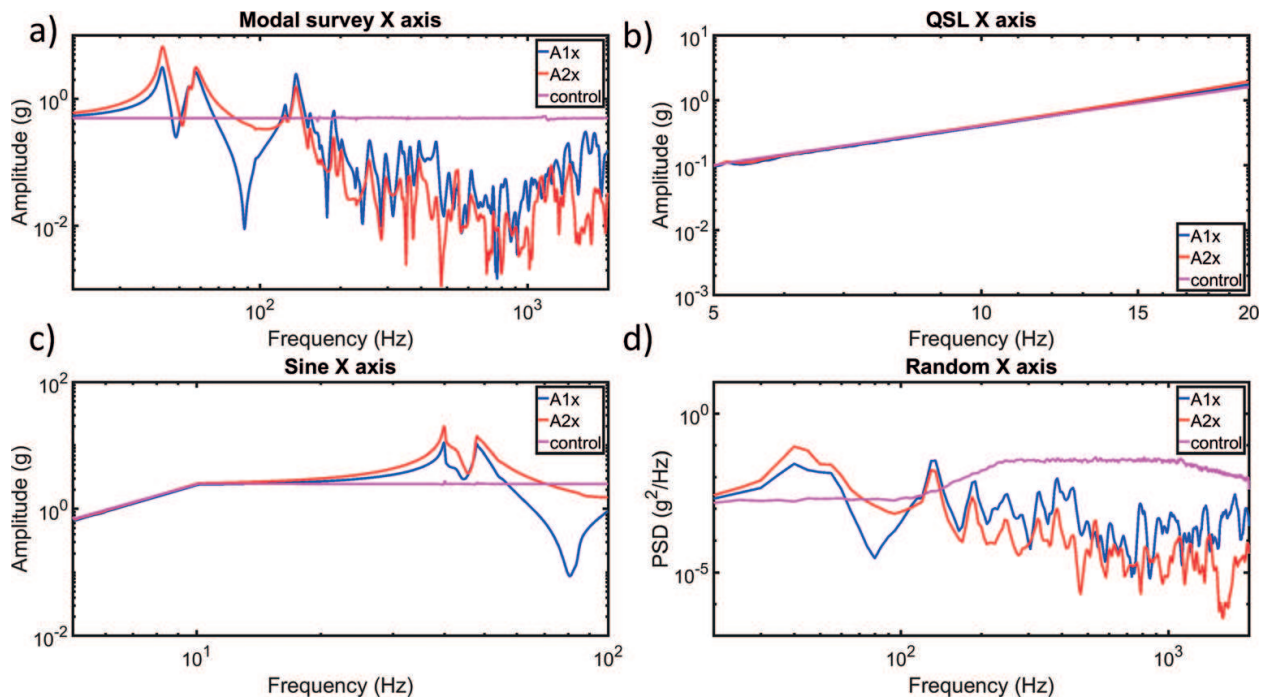


Figure 10. Results of the tests in the X-axis. (a) Modal survey, (b) QSL, (c) sine vibration, and (d) random vibration.

line represents the signal of the accelerometer 1 in the longitudinal axis, the blue color line represents the accelerometer 2 in the longitudinal axis, and the magenta line represents the control signal. **Table 2** summarizes the results obtained with the modal survey tests before and after the QSL, sine, and random tests were done. All the values are provided with the measurements of accelerometer 1 since the values provided by accelerometer 2 did not differ significantly.

With the modal survey, all the modes were characterized. The first mode was the most representative. This was located at 43.19 Hz. The amplitude of the first mode was 3.22 g. For comparison, the main mode of the structure manufactured by CNC in aluminum had a frequency of 190.77 Hz and had an amplitude of 8.2 g. This shows that the 3D-printed structure has less rigidity, but it still fulfills the requirement provided by the PSLV launcher authority, which established that the first mode of the spacecraft shall be higher than 20 Hz.

3D-printed ULTEM™ structural model—modal survey results before and after the quasi-static load, sine, and random vibration tests in the X-axis

	Pre-QSL	Post-QSL	Pre-sine	Post-sine	Pre-random	Post-random
First modal freq. [Hz]	43.19	43.19	43.19	40.55	40.55	40.55
Observed deviation	<0.1%		-6.10%		<0.1%	
Accel. peak [g]	3.22	3.33	3.33	2.74	2.74	2.71
Observed deviation	3.40%		-6.10%		-1.8%	

Table 2. Results of the modal survey tests before and after the QSL, sine, and random vibration tests in the X-axis.

The QSL test indicated that the structure behaved perfectly. There was neither representative excitation nor attenuation in the structure. It perfectly followed the control signal without passing the limit values established by the control. After this test was finished, the modal survey showed that there was no significant deviation of the modes. The amplitude of the first mode was increased to 3.33 g (3.40% more).

The sine vibration test showed that the structural model entered in resonance at the frequencies of the first and the second modes. After this test, the first mode slightly changed the frequency to 40.55 Hz and reduced the amplitude to 2.74 g (6.10% less). This represented no major changes in the structure.

In the random vibration test, all the modes were excited. After the test, the frequency of the first mode did not change (40.55 Hz). Its amplitude was slightly reduced to 2.71 g (1.8% less).

There were no shifts over 10% in the frequency of the first mode before and after all the specific tests. In addition, after all the tests, the structure was analyzed, and no visible changes were identified (plastic deformation, broken screws, lost screws, and unassembled parts, among others), which means that all the tests were successfully passed.

3.2. Y-axis test results of the 3D-printed ULTEM™ structure

Figure 11 shows the results for the test carried out in the Y-axis of the 3D-printed ULTEM™ structural model: modal survey (**Figure 11(a)**), QSL (**Figure 11(b)**), sine (**Figure 11(c)**), and random vibration (**Figure 11(d)**) tests. The red color line represents the signal of the accelerometer 1 in the longitudinal axis, the blue color line represents the accelerometer 2 in the longitudinal axis, and the magenta line represents the control signal. **Table 3** summarizes the

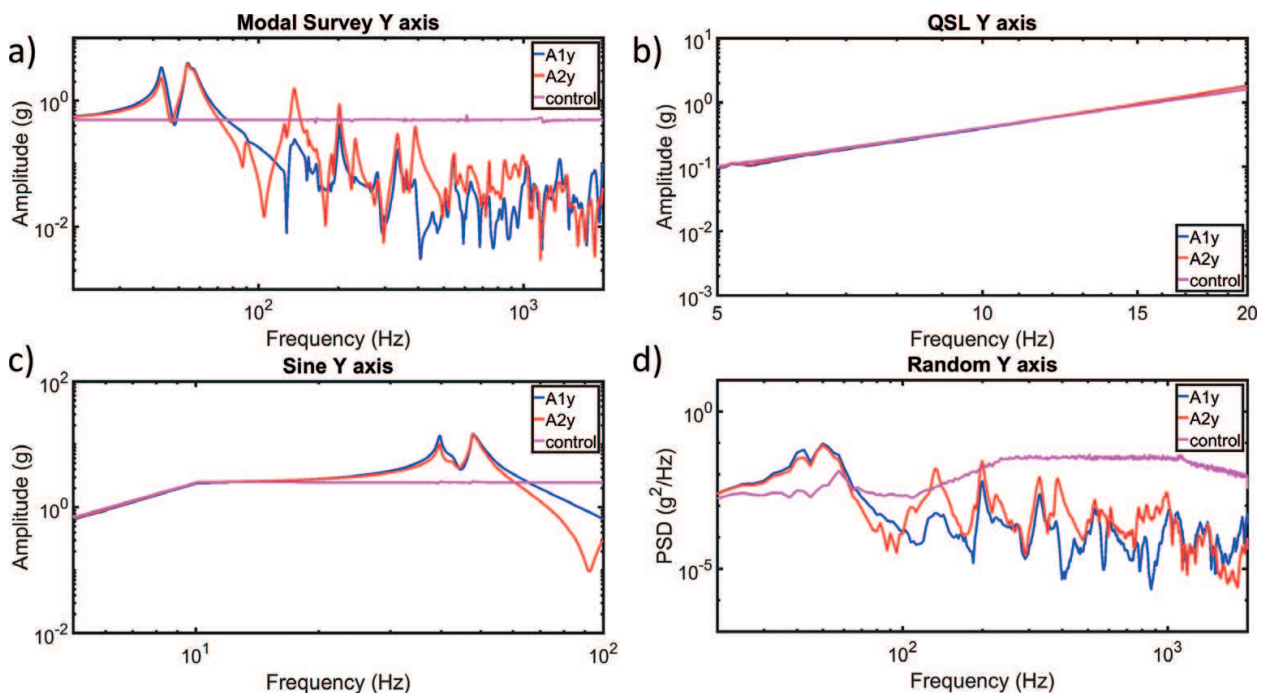


Figure 11. Results of the tests in the Y-axis. (a) Modal survey, (b) QSL, (c) sine vibration, and (d) random vibration.

3D-printed ULTEM™ structural model—modal survey results before and after the quasi-static load, sine, and random vibration tests in the Y-axis

	Pre-QSL	Post-QSL	Pre-sine	Post-sine	Pre-random	Post-random
First modal freq. [Hz]	43.19	43.19	43.19	41.66	41.66	41.66
Observed deviation	<0.1%		-3.70%		<0.1%	
Accel. peak [g]	3.44	3.54	3.54	3.18	3.18	3.08
Observed deviation	2.90%		-10.20%		-3.10%	

Table 3. Results of the modal surveys tests before and after the QSL, sine, and random vibration tests in the Y-axis.

results obtained with the modal survey tests before and after the QSL, sine, and random tests were done. As in the tests done in the X-axis, all the values are provided with the measurements of accelerometer 1 since the values provided by accelerometer 2 did not differ significantly.

With the modal survey, all the modes were characterized. The first mode was located at 43.19 Hz. The amplitude of the first mode was 3.44 g. For comparison, the main mode of the structure manufactured by CNC in aluminum had a frequency of 190.63 Hz and had an amplitude of 5.88 g.

Again, in the QSL test, the structure behaved perfectly between the margins defined by the control. The modal survey after this test showed that there was no significant deviation of the modes. The amplitude of the first mode was slightly increased to 3.54 g.

The sine vibration test showed that the structural model entered in resonance at the frequencies of the first and the second modes. After this test, the first mode slightly changed the frequency to 41.66 Hz and reduced the amplitude to 3.18 g (at 10.20% less, which indicates that the components of the structure would be less accelerated because the structure gained damping). This represented no major changes in the structure but an increase in the damping.

In the random vibration test, all the modes were excited. However, the first mode did not change in frequency, and the amplitude was reduced at 3.10% to 3.08 g.

There were no shifts over 10% in the frequency of the first mode before and after all the specific tests. In addition, after all the tests in the Y-axis, the structure was analyzed, and no visible changes were identified, which means that all the tests were successfully passed.

3.3. Z-axis test results of the 3D-printed ULTEM™ structure

Figure 12 shows the results for the test carried out in the Z-axis of the 3D-printed ULTEM™ structural model: modal survey (**Figure 12(a)**), QSL (**Figure 12(b)**), sine (**Figure 12(c)**), random vibration (**Figure 12(d)**), and shock (**Figure 12(e)**) tests. The red color line represents the signal of the accelerometer 1 in the longitudinal axis, the blue color line represents the accelerometer 2 in the longitudinal axis, and the magenta line represents the control signal. **Table 4** summarizes the results obtained with the modal survey tests before and after the QSL, sine, random,

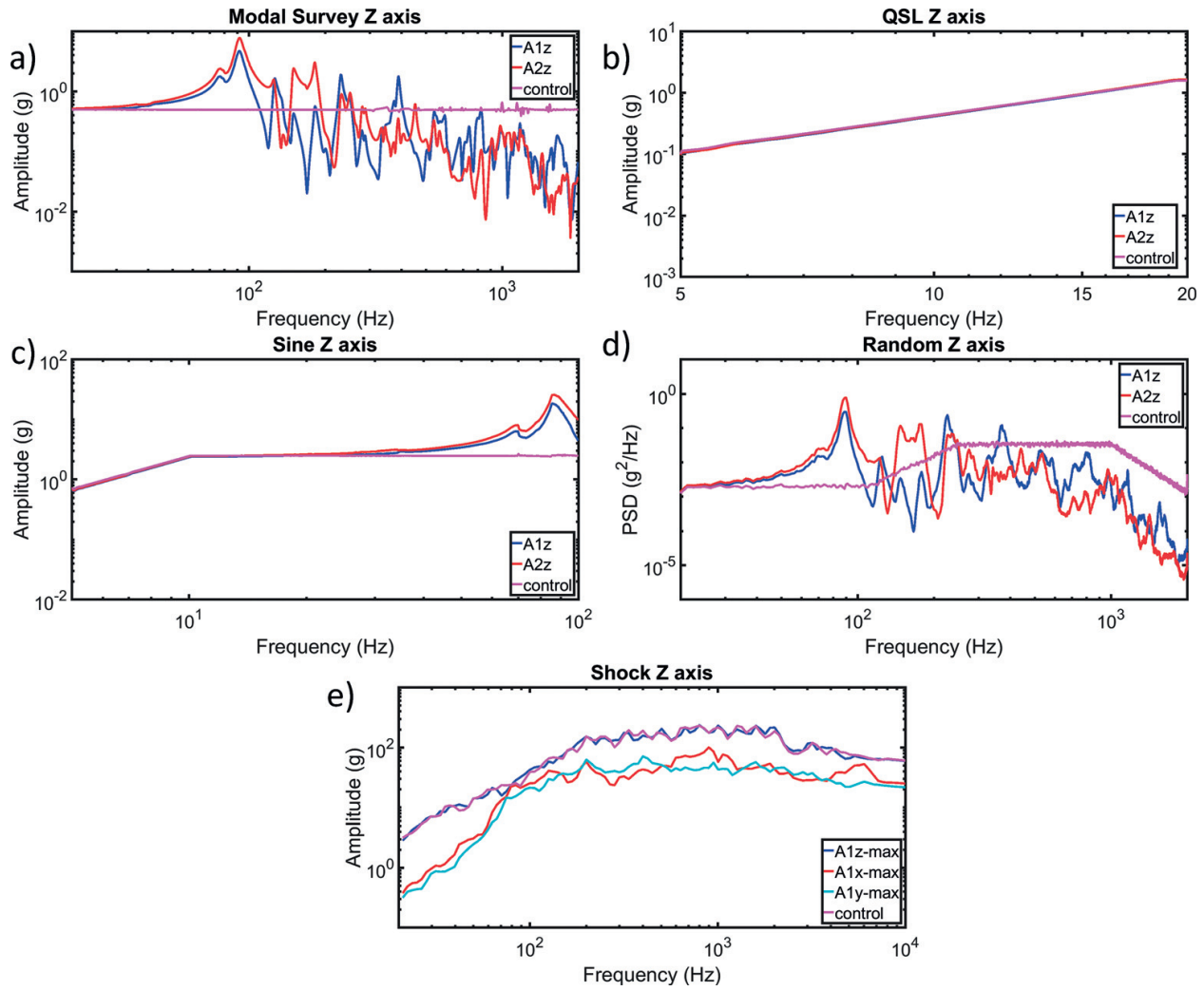


Figure 12. Results of the tests in the Y-axis. (a) Modal survey, (b) QSL, (c) sine vibration, (d) random vibration, and (e) shock.

3D-printed ULTEM™ structural model – modal survey results before and after the quasi-static load, sine, and random vibration tests in the Y-axis

	Pre-QSL	Post-QSL	Pre-sine	Post-sine	Pre-random	Post-random	Pre-shock	Post-shock
First modal freq. [Hz]	77.19	77.3	77.3	74.46	74.46	74.46	74.46	73.79
Observed deviation	0.14%		-3.70%		<0.1%		-0.90%	
Accel. peak [g]	1.79	2.12	2.12	1.7	1.7	1.67	1.67	1.64
Observed deviation	18.40%		-19.80%		-1.80%		-1.80%	

Table 4. Results of the modal survey tests before and after the QSL, sine, random vibration, and shock tests in the Z-axis.

and shock tests were done. As in the tests done in the X and Y axes, all the values are provided with the measurements of accelerometer 1 since the values provided by accelerometer 2 did not differ significantly.

With the modal survey, all the modes were characterized. The first mode was located at 77.19 Hz. The amplitude of the first mode was 1.79 g. For comparison, the main mode of the structure manufactured by CNC in aluminum had a frequency of 354.45 Hz and had an amplitude of 4.00 g.

In the QSL test, the structure behaved perfectly between the margins defined by the control. The modal survey after this test showed that the first mode changed the frequency to 77.3 Hz (0.14%). The amplitude was increased to 2.12 g (18.40%). This represented no major changes in the structure but an increase in the stiffness.

The sine vibration test showed that the structural model entered in resonance at the frequency of the first mode. After this test, the first mode slightly changed the frequency to 74.46 Hz (3.70% lower) and reduced the amplitude to 1.70 g (at -19.80% less). This represented no major changes in the structure but an increase in the damping.

In the random vibration test, all the modes were excited. After the test, the first mode did not change (74.46 Hz). Its amplitude was reduced to 1.67 g (1.80% less).

In the shock vibration test, the structure behaved well. After the test, the first mode had a frequency of 73.79 Hz (0.90% less), and its amplitude was reduced to 1.64 g (1.80% less).

There were no significant changes in the structure, defined by shifts over 10% in the frequency of the first mode, before and after the tests. The visual analysis of the structure did not provide any change, which means that all the tests in this axis were successfully passed. Since the structure passed all the tests in all three axes, the structure was considered to be qualified to fly in the PSLV launcher.

3.3.1. Robustness test results

The robustness test was done with the random vibration test as the baseline due to its wider frequency range. First of all, the test level was raised up to the test specification provided by the GSFC General Environmental Verification Standard (GEVS) [13]. Following the same philosophy as for the regular test, a modal survey was carried out before and after the random test. An interactive process was started by increasing the load up step-by-step, with their corresponding modal surveys until a failure occurred. The levels of the robustness test can be seen in **Figure 13(a)**. The original profile of the PSLV random vibration test is represented in blue, the GEVS profile is represented in red, the extended profile of the second iteration is represented in magenta, and the profile at which the structure fails is represented in cyan.

Contrary to the expected failure by breaking a bolt by excessive shear stress, the failure was a combination of HeliCoil extractions by excessive traction stress and two cracks in one of the corners near the fixing point in contact with the shaker. Obviously, some bolts were bended after the failure as a side effect of the part cracks, but any of them was broken.

Figure 13(b) shows a comparison of the modal survey done before executing the test which modified the 3D-printed ULTEM™ structural model (blue signal) and after the execution of that random vibration test (red signal). The control signal is represented in magenta.

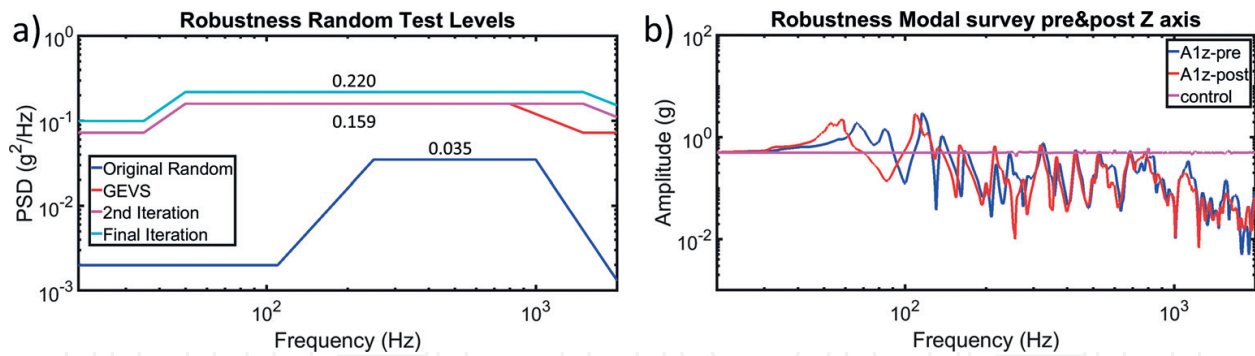


Figure 13. Robustness test levels and results. (a) Test level of the robustness test and (b) modal survey before and after the last random vibration test.

After the test the modes of the structural model are substantially shifted to the left, i.e., to lower frequencies: the first mode shifted from 53.10 to 66.19 Hz, which represented a change of 19.78% (clearly over 10%). The amplitude of the signal slightly changed from 1.95 g before the test to 1.91 after the test (2.05%). Besides, the shape of the signal also changed. After the test, the first and the second modes are nearer. This represents a significant change in the structure at the level of the test, and as conclusion, it is not passed. However, the structure was taken to the limit, which was much higher than the qualification levels.

4. Discussion

The 3D-printed ULTEM™ structural model widely fulfilled the requirements imposed by the PSLV launcher authority, which enables the technology tested to be used in space and more specifically in the functional structure of satellites.

By comparing the characteristics of the validated technology with respect to the classical CNC milling in aluminum alloy, the 3D-printed model presented a clearly different behavior. In **Figure 14**, the modal survey obtained in the two structural models was represented to facilitate comparison. There was a clear difference in the rigidity of the two materials with the same geometry. The 3D-printed model had natural modes with lower frequencies than the CNC structure in aluminum. This implies more flexibility and, as a result, larger displacements. Damages could be found if the structure is displaced, which would cause damages in the satellite components. Damages could also be found if the structure is impacted by an external item in the launcher. This result was expected as previous studies in the mechanical properties suggest a tensile modulus of 2 GPa for ULTEM™ parts made by FDM [14]. When this value is compared with aluminum typical value for tensile modulus (70 GPa), a simplified mass-spring model foresees a reduction in the first mode frequency of 80% which is coherent with the test results. In consequence the manufacturing flaws described in [14] do not have a remarkable impact in functional parts as the stiffness does not seem to be affected and the catastrophic fail was due to a stress concentration near the structure corners not to a manufacturing defect. In conclusion both the material and the manufacturing method have been proven to be valid for their use in primary structural application despite the local manufacturing flaws.

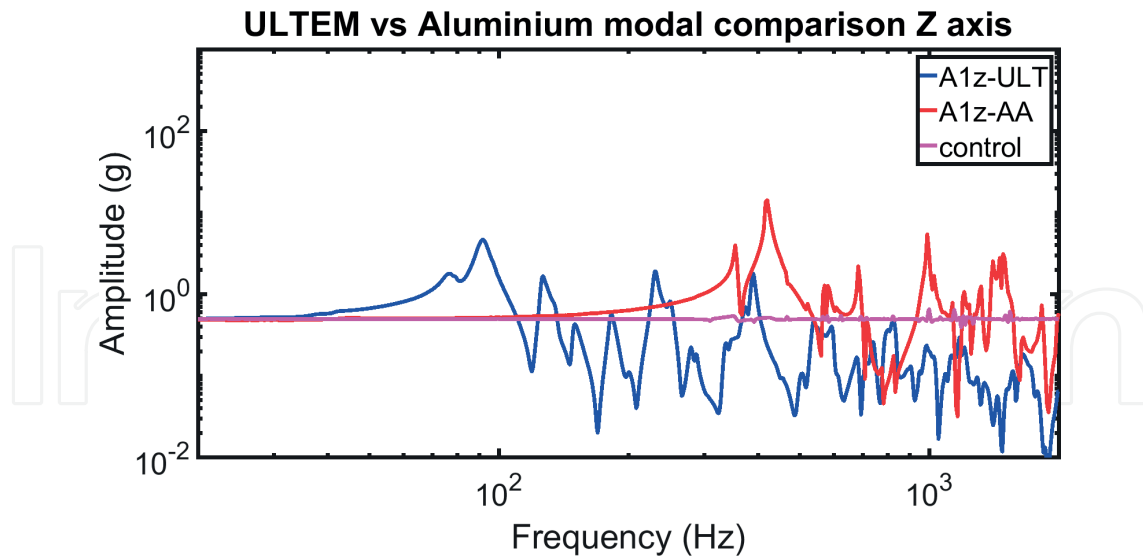


Figure 14. 3D-printed ULTEM™ structural model vs. CNC-milled aluminum structural model comparison.

In terms of damping, as can also be seen in **Figure 14**, the ULTEM™ model had a significant higher damping leading to a less sharp modal survey profile. This effect could be especially beneficial for all the electronic components inside the satellite as most of the vibration energy was dissipated by the structure, thus reducing the effective acceleration that those components could suffer. Primarily in the response to high frequency, associated with a higher energy, which can cause a higher damage in the electronic components such as relays or oscillators, this attenuation is desirable, and it can be considered as a thermoplastic structure advantage [15].

5. Conclusions

In this work, the structure of a satellite which was made in 3D-printed ULTEM™ was validated. A structural model with realistic mass dummies was tested under qualification levels established by the PSLV launcher authority. The tests were successfully passed, which indicate that the proposed structure was apt to be put in orbit.

Besides, the structure was compared with that manufactured with a classical CNC approach in aluminum alloy. The results indicate that the 3D-printed structure has less rigidity and more damping than the CNC aluminum structure. This can be beneficial for electromechanical components of the satellites since the ULTEM™ structure acts as a low-pass filter. However, it has larger displacements, which has to be considered in order to avoid impacts between components and external surfaces of the satellite.

In addition, during the experimentation of both the 3D-printed and the CNC-milled models, some ULTEM™ and aluminum powder were generated because of the stress caused by the trials. This powder generation and the effect that it could have over optical components in the satellite are still to be analyzed in depth. In addition, the thermal-vacuum cycling and atomic oxygen effects have to be studied before flying this structure in the space environment.

Acknowledgements

The research leading to these results has received funding from the Horizon 2020 Program of the European Union's Framework Programmes for Research and Innovation (H2020-PROTEC-2015) under REA grant agreement number 687500-ReDSHIFT (<http://redshift-h2020.eu/>).

Conflict of interest

This publication reflects only the author's views, and the European Commission is not liable for any use that may be made of the information contained therein.

Author details

Jonathan Becedas*, Andrés Caparrós, Antonio Ramírez, Pablo Morillo, Esther Sarachaga and Almudena Martín-Moreno

*Address all correspondence to: jonathan.becedas@elecnor-deimos.com

Elecnor Deimos Satellite Systems, Puertollano, Spain

References

- [1] Messier D. What a ride to space costs these days. Parabolic Arc. 2017. Available from: <http://www.parabolicarc.com/2017/08/18/ride-space-costs-days/> [Accessed: Jun 6, 2018]
- [2] Gstattenbauer GJ. Cost comparison of expendable, hybrid, and reusable launch vehicles [thesis]. Ohio: Department of the Air Force, Air University, Air Force Institute of Technology, Wright-Patterson Air Force Base; 2004
- [3] Spaceflight, Pricing information. 2018. Available from: <http://spaceflight.com/schedule-pricing/#pricing> [Accessed: Jun 6, 2018]
- [4] Wassmer W. The materials used in artificial satellites and space structures. Azo Materials. 2015. Available from: <https://www.azom.com/article.aspx?ArticleID=12034> [Accessed: Jun 6, 2018]
- [5] Molitch-Hou M. Made In Space Begins 3D Printing PEI/PC on the ISS. Engineering.com. 2017. Available from: <https://www.engineering.com/3DPrinting/3DPrintingArticles/ArticleID/15254/Made-In-Space-Begins-3D-Printing-PEIPC-on-the-ISS.aspx> [Accessed: Jun 6, 2018]
- [6] Mudarra M, Sellarès J, Cañadas JC, Diego JA. Sublinear dispersive conductivity in polyetherimides by the electric modulus formalism. IEEE Transactions on Dielectrics and Electrical Insulation. 2015;**22**(6):3327-3333

- [7] ECSS Secretariat, ESA-ESTEC, Requirements & Standards Division. ECSS-E-ST-10-03C, Space Engineering-Testing, ESA Publications Division, Noordwijk, The Netherlands. Issue 2. Jun 1, 2012
- [8] Yilmaz F, Haktanir OO, Uygur AB. Quasi-static structural test of satellites. In: 7th International Conference on Recent Advances in Space Technologies (RAST), Istanbul, Turkey: IEEE; 16–19 June, 2015
- [9] Department of Space Indian Research Organisation. Polar Satellite Launch Vehicle. Government of India. n.d. Available from: <https://www.isro.gov.in/launchers/pslv> [Accessed: Jul 6, 2018]
- [10] ECSS Secretariat, ESA-ESTEC, Requirements & Standards Division. ECSS-E-ST-10-02C, Space Engineering-Verification, ESA Publications Division, Noordwijk, The Netherlands. Mar 6, 2009
- [11] Roethlisberger G. Phase C Launch Environment, Ref.: S3-C-STRU-1-6-Launch Environment.doc. EPFL Lausanne Switzerland. 2008. Available from: <http://www.goldstem.org/Swiss%20Cube/09%20-%20Structures%20and%20configuration/S3-C-STRU-1-6-Launch%20Environment.pdf> [Accessed: Jul 6, 2018]
- [12] 6U CubeSat Design Specification, The CubeSat Program, Cal Poly SLO, California, USA. 2016. Available from: https://static1.squarespace.com/static/5418c831e4b0fa4ecac1bacd/t/573fa2fee321400346075f01/1463788288448/6U_CDS_2016-05-19_Provisional.pdf [Accessed: Jul 6, 2018]
- [13] NASA Goddard Space Flight Center. General Environmental Verification Standard (GEVS) for GSFC Flight Programs and Projects. NASA Goddard Space Flight Center, Greenbelt, Maryland. 2013. Available from: <https://standards.nasa.gov/standard/gsfsc/gsfsc-std-7000> [Accessed: Jul 11, 2018]
- [14] Bagsik A, Schöppner V, Klemp E. FDM part quality manufactured with Ultem* 9085. In: 14th International Scientific Conference on Polymeric Materials. Martin-Luther-Universität Halle-Wittenberg, 15–17 September, Halle (Saale), Germany, Vol. 15. 2010. pp. 307-315
- [15] Veprik AM, Babitsky VI. Vibration protection of sensitive electronic equipment from harsh harmonic vibration. *Journal of Sound and Vibration*. 2000;238(1):19-30

